Effect of pressure on molecular photodissociation in matrices: Molecular dynamics simulations of Cl_2 in Xe

R. Alimi
Department of Physical Chemistry and the Fritz Haber Center for Molecular Dynamics, The Hebrew University of Jerusalem, Jerusalem 91904, Israel

V. A. Apkarian and R. B. Gerber[a)]
Department of Chemistry, University of California, Irvine, California 92717

(Received 17 December 1991; accepted 15 September 1992)

A theoretical study is presented on the photodissociation dynamics of Cl_2 in crystalline xenon at 100 K, and within a range of pressure between 0 and 100 kbar. Temperature/pressure ensemble molecular dynamics simulations were carried out. The potentials used were accurate enough to reproduce the experimental equation of state of solid xenon. The results show that the photodissociation quantum yield varies strongly with pressure, falling from 30% at zero pressure, to 2% at 12.5 kbar, and 0% at higher pressures. These yields are in good agreement with experimental measurements. This behavior is found to be due to the strong effect of pressure on the librational (rotational) amplitudes of the Cl_2 molecule and to the sharp dependence of the photodissociation yield on the molecular orientation in the reagent cage.

I. INTRODUCTION

The photodissociation of diatomic molecules in rare-gas crystals provides an attractive and fundamental model framework for exploring basic problems of condensed phase reaction dynamics. Both experimental and theoretical studies of such systems have been recently reported.[1–5] This includes quantitative comparisons between experiments and classical molecular dynamics (MD) simulations.[6–7] Such comparisons are obviously of major importance for developing a first-principles understanding of these condensed-matter reactions. The reactions dynamics in a condensed matter system may depend, in general, on dynamical parameters such as the photodissociation energy and on the thermodynamic parameters, pressure, and temperature being the most relevant choices for the latter. Theoretical studies of photodissociation in matrices have focused on the role of the photodissociation energy[6,7] and, to some extent, of temperature.[1,3,7,8] The question of the role of pressure was not hitherto explored theoretically and such a study is our aim here. In previous studies of reactions in solids considerable attention has been already given to the photodynamics of Cl_2 trapped in crystalline xenon[8–11] and other rare-gas matrices. Bondybey and coworkers[12] have shown that at the temperatures and wavelengths they studied, a very strong cage effect in Ar and Kr matrices prevents photodissociation of the chlorine molecule. Having excited the halogen molecule from its electronic ground state to the first neutral excited repulsive $^1\Pi_u$ state, these authors always observed 100% recombination. More recent studies[10,11] have demonstrated that dissociation via charge-transfer (harpooning) mechanisms is, however, a very efficient process even at low temperatures. The dynamics of the photoinduced Cl–Cl separation in these ionic channel harpooning processes was found to be promoted by hole (positive charge) migration among the Xe atoms in the vicinity of the Cl_2.

Extensive MD simulations of the Cl_2 photolysis in solid xenon in the neutral channel have been performed.[8] These calculations have shown that nearly complete recombination at temperatures less than 90 K occurs due to unfavorable initial alignment of the molecule in its trapping site. The initial orientations are such that upon photoadsorption into the repulsive state each of the Cl atoms strikes a Xe atom (rather than a "transition state" for cage exit), loses part of its energy and ultimately recombination occurs. Above 90 K nearly free rotation of the Cl_2 appears and the photodissociation quantum yield suddenly increases. At 100 K a reaction probability of about 30% can be measured. Unfortunately, experimental confirmation of the theoretical predictions was until recently difficult to obtain under standard conditions. At temperatures around 100 K, self-diffusion induces the clustering of impurities which prevents studies of the isolated species. In a recent paper, Katz and Apkarian[13] have used a diamond-anvil cell to reach ultrahigh pressures where the crystal remains perfect even at room temperature. At all studied pressures (2–10 GPa) and temperatures (30–300 K), no direct dissociation of Cl_2 at 308 nm via the $^1\Pi_u$ channel was observed. This strongly motivates the need for theoretical calculations of photodissociation at high pressure. The present paper aims at filling the gap between the experimental and theoretical studies of the process by varying the pressure in the MD calculations. Comparison between theory and experiment will then be presented.

Although the choice of the thermodynamic ensemble is merely a matter of convenience in the thermodynamic limit, this is not the case for the finite size systems one has to deal with in computer simulations. The natural choice for MD is a microcanonical ensemble (number, volume, energy—NVE). Any other choice would require changing

[a)]Also at: Department of Physical Chemistry and the Fritz Haber Center for Molecular Dynamics, The Hebrew University of Jerusalem, Jerusalem 91904, Israel.

 0021-9606/93/010331-5$06.00

the equations of motion, introducing some auxiliary parameters or artificial degrees of freedom. Several methods have been developed to perform isothermic and isobaric classical trajectories (for a good review and description see Ref. 14). In the *extended system method*,[15,16] the basic idea is to couple the system to an external reservoir by adding another degree of freedom. The reservoir has a thermal inertia Q. The main problem lies in the arbitrariness of the choice of Q. A small Q leads to rapid box oscillations while a high mass results in a poor exploration of the phase space. The *constraint method*[17] modifies the Newton equations of motion by adding constraints to keep T and P constant. Unfortunately, the method is numerically unstable and relatively time consuming. The method we have chosen is based on a weak and fully tunable coupling to a external bath.[18] Neither additional, artificial degrees of freedom, nor modifications of the usual equations of motion are required. The scheme is stable, easy to program, and does not increase significantly the computational time. As far as we are aware, this is the first use of a P-T ensemble in the study of chemical reaction dynamics (as opposed to equilibrium properties) in condensed matter.

The outline of the paper is as follows. Section II describes, in detail, the system, the potentials, and the methods used in the calculations. In Sec. III the results are presented and discussed. Section IV outlines conclusions.

II. SYSTEM AND METHODS

The sample used in the MD simulations reported here consists of a Cl_2 molecule embedded in a slab of 108 Xe atoms. Initially, these atoms were arranged in a perfect fcc structure and the center of mass of the molecule replaces one of the rare-gas atoms. However, MD simulations were used to allow for the structural relaxation of this system. Periodic boundary conditions are imposed. Convergence with respect to the size of the sample was tested and confirmed by increasing the sample to 257 atoms.

Starting from an initial configuration of 0 K and zero pressure and in the electronic ground state (before photodissociation), the system was first equilibrated to the desired temperature and pressure. From this equilibrium state, 200 configurations were selected as the system evolved in time in order to reasonably sample initial configurations and velocities in the number-pressure-temperature (NPT) ensemble. Each of these 200 configurations serves as an initial condition for the photodissociation of the halogen molecule.

Since the pressure is a very sensitive function of the potential, the Xe–Xe interaction has to be chosen extremely carefully. Barker *et al.*[19] have reported a very accurate Xe–Xe potential. It has the form

$$u(r)=\epsilon[u_0(r)+u_1(r)], \tag{1}$$

where

$$u_0(r)=\sum_{i=0}^{5} A_i(r-1)^i e^{\alpha(1-r)}-\sum_{i=0}^{2}\frac{C_{6+2i}}{r^{6+2i}+\delta} \tag{2}$$

and

TABLE I. Potential parameters. The two first lines refer to the Xe–Xe potential; the others to the Cl–Cl interaction.

ϵ^*	R_m^{**}	R_0^{**}	A_0	A_1	A_2	A_3	A_4	A_5	C_6	C_8	C_{10}	α	δ	P	Q	α'
0.558	4.36	3.89	0.24	−4.81	−10.9	−25.0	−50.7	−200.	1.05	0.16	0.03	12.5	0.01	59.3	71.1	12.5

ϵ^*	r_m^{**}	β_1	β_2	C_6^{***}	C_8^{***}	x_1	x_2	a_1	a_2	a_3	a_4
0.81	3.23	5.2	3.3	2279.	14250.	1.21	1.65	−0.75	1.65	0.4434	−2.5063

(*) kcal/mol (**) Å (***) kcal/mol $Å^{6,8}$

$$u_1(r)=[P(r-1)^4+Q(r-1)^5] \quad \text{if} \quad r>1,$$

$$u_1(r)=0 \quad \text{if} \quad r<1, \tag{3}$$

where ϵ is the depth of the potential at the minimum R_m and $r=R/R_m$, R being the internuclear distance. The parameters are summarized in Table I. Because of its complexity the potential was tabulated and a very fast interpolation procedure[20] was employed to evaluate the forces between the tabulated values.

In order to check the accuracy of the potential we have computed and compared to experimental data the variations of the lattice parameter of the xenon lattice as a function of the pressure applied to the system at 100 K. Figure 1 shows that we were able to reproduce very well the experimental equation of state[21] of solid xenon at 100 K.

The Cl_2 ground-state potential can be represented by a Morse function[22]

$$V(r)=\epsilon(e^{-2\beta(r-r_e)}-2e^{-\beta(r-r_e)}) \tag{4}$$

with $\epsilon=2.475$ eV, $\beta=2.036$ A, and $r_e=1.988$ A. The excited repulsive potential that the Cl_2 molecule reaches after a vertical transition is a $^1\Pi_u$ state. Its form was chosen to fit the data given by Peyerimhoff *et al.*[23] The vertical electronic energy from the ground to the electronic state is 4.05 eV, which corresponds to an excess energy of ≈ 1.3 eV for the photofragments. This energy fits the experimental 308 nm excitation wavelength. We assumed that after the ex-

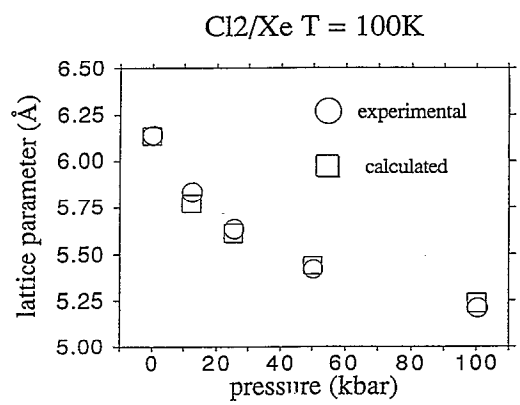

FIG. 1. The lattice parameter of a xenon lattice at 100 K as a function of the pressure, theory vs experiment.

citations took place the interactions between Cl_2 and Xe are given by a sum of previous Cl/Xe atom–atom potentials.

For the Cl/Xe interaction the crossed molecular beam potential obtained by Becker *et al.*[24] were used. The potential is given by a Morse–Morse–Hermite spline–Van der Waals reduced function:

$$\begin{aligned} &f(x)=V/\epsilon, \quad x=r/r_m \\ &f(x)=e^{2\beta_1(1-x)}-e^{\beta_1(1-x)}, \quad 0\leqslant x\leqslant 1 \\ &f(x)=e^{2\beta_2(1-x)}-e^{\beta_2(1-x)}, \quad 1\leqslant x\leqslant x_1 \\ &f(x)=a_1+(x-x_1)\{a_2+(x-x_1)[a_3+a_4(x-x_1)]\}, \\ &\qquad x_1<x<x_2 \\ &f(x)=\frac{C_{6R}}{x^6}-\frac{C_{8R}}{x^8}, \quad x_2\leqslant x<\infty, \end{aligned} \tag{5}$$

where $C_{iR}=C_i/\epsilon r_m^i$. The parameters are listed in Table I. The analytic form of the potential is complex and tabulation and interpolation were found to be the optimal solution for computing efficiently all the required Xe/Cl interactions.

Before describing the method of generating the NPT ensemble, we define the temperature and the pressure of the system. If $\mathbf{H}$ is the Hamiltonian of the system, p_k and m_k the momentum and the mass of atom k, respectively, N the number of degrees of freedom, and k_B the Boltzmann constant, then we have, from the virial theorem,

$$\left\langle p_k \frac{\partial \mathbf{H}}{\partial p_k} \right\rangle = k_B T. \tag{6}$$

This gives

$$\left\langle \sum_{i=1}^{N} \frac{|\mathbf{p}_i|^2}{2m_i} \right\rangle = 3Nk_B\mathbf{T}/2 \tag{7}$$

which provides the instantaneous (fluctuating) temperature function

$$\mathbf{T}=\frac{2}{3Nk_B}\sum_{i=1}^{N}\frac{|\mathbf{p}_i|^2}{2m_i} \tag{8}$$

For the pressure, one starts again from the virial theorem

$$\left\langle q_k \frac{\partial \mathbf{H}}{\partial q_k} \right\rangle = k_B T \tag{9}$$

using Hamilton equations of motion one gets

$$-\frac{1}{3}\left\langle \sum_{i=1}^{N} \mathbf{r}_i \cdot \nabla_{\mathbf{r}_i} V \right\rangle = \frac{1}{3}\left\langle \sum_{i=1}^{N} \mathbf{r}_i \cdot \mathbf{f}_{\text{total},i} \right\rangle = -Nk_B T, \tag{10}$$

where V is the potential energy and $f_{\text{total},i}$ includes both intermolecular and external forces acting on particle i. The latter are related to the pressure by

$$\frac{1}{3}\left\langle \sum_{i=1}^{N} \mathbf{r}_i \cdot \mathbf{f}_{\text{external},i} \right\rangle = -PV, \tag{11}$$

where V is the volume of the system. Defining the internal virial W by

$$-\frac{1}{3}\sum_{i=1}^{N}\mathbf{r}_i\cdot\nabla_{\mathbf{r}_i}\mathbf{V}=\frac{1}{3}\sum_{i=1}^{N}\mathbf{r}_i\cdot\mathbf{f}_{\text{internal},i}=\mathbf{W} \tag{12}$$

then

$$PV=Nk_BT+\langle\mathbf{W}\rangle \tag{13}$$

from what one can extract the instantaneous pressure $\mathbf{P}$

$$\mathbf{P}=\rho k_B\mathbf{T}+\mathbf{W}/V \tag{14}$$

and if only pairwise interactions are considered then

$$\mathbf{W}=-\frac{1}{3}\sum_{i}\sum_{j>i} w_{ij}(r_{ij}), \quad \text{with } w_{ij}=r\frac{dv_{ij}}{dr} \tag{15}$$

which completes the definition of the pressure (v_{ij} is the pair potential between particles i and j).

Let us now discuss briefly the scheme we used to generate the NPT ensemble. One can show that starting from a Langevin type equation of motion, one gets a temperature time evolution

$$\left(\frac{dT}{dt}\right)_{\text{bath}}=2\gamma(T_0-T), \tag{16}$$

where T_0 is the desired constant temperature and $\tau_T=1/2\gamma$ is a tunable coupling time. This finally leads to a scaling factor of the velocity vectors from v to λv with

$$\lambda=\left[1+\frac{\delta t}{\tau_T}\left(\frac{T_0}{T}-1\right)\right]^{1/2}. \tag{17}$$

For the pressure, one starts by a similar equation

$$\left(\frac{dP}{dt}\right)_{\text{bath}}=\frac{(P_0-P)}{\tau_P} \tag{18}$$

this finally leads to a proportional scaling of the position vectors per time step from $\mathbf{r}$ to $\mu^{1/3}\mathbf{r}$ with

$$\mu=1-\frac{\beta_T\delta_t}{\tau_P}(P_0-P), \tag{19}$$

where β_T is the isothermal compressibility and δ_t the time interval at which the scaling is done. The numerical values of the bath relaxation times τ_T and τ_P are chosen to lead to a "smooth" response of the system to the constraints of constant temperature and/or pressure. Rapid convergence and numerical stability of the integration scheme govern the choice of these parameters and the choice can change with time. The typical range of τ_T and τ_P was between 10^{-13} and 10^{-10} s depending mainly on the desired temperature and pressure of the system. It should be emphasized that the constraints of constant P and T were applied only to the description of the equilibrium system prior to photoexcitation. Upon photodissociation, the time evolution of the system was calculated by the usual NVE ensemble molecular dynamics. This prevents any introduction of unphysical effects in the excited state dynamics, due to the constraints involved in the constant P and T algorithms.

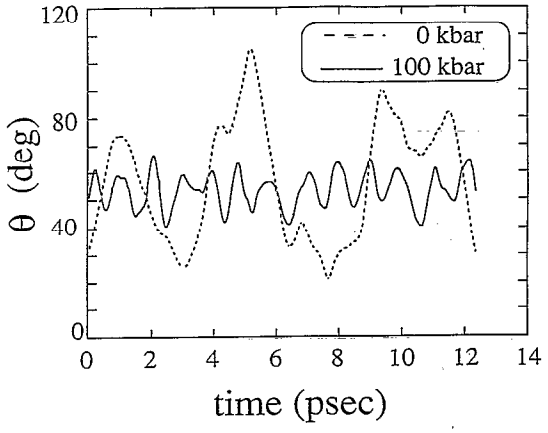

FIG. 2. The time evolution of the angle θ at 100 K for two extreme pressure values.

III. RESULTS

All the calculations were done for a system at 100 K, varying the pressure from 0 to 100 kbar (i.e., from 0 to 10 GPa), which corresponds to the experimental range of pressures studied in Ref. 13. We first consider the Cl_2 molecule before the excitation while it is still in the electronic ground state. From an equilibrated system we have recorded the variations of the angle θ between a fixed axis and the molecular bond axis. This angle basically measures the deviations from an equilibrium orientation of the halogen in its trapping site prior to photodissociation. In a previous study of the same system,[8] we have shown that at low temperatures the molecule is locked in its lowest librational state, while free rotation is expected to appear only at $T > 90$ K. Figure 2 shows the time evolution of θ for two extreme pressure values. At zero pressure one can recognize the onset of free rotation mentioned earlier. However, at 100 kbar, θ exhibits small fluctuations around an equilibrium position. Such a behavior is very similar to what we have observed at zero pressure at very low temperatures. The Cl_2 molecule is locked by the pressure in a narrow librational potential well. A close examination of the geometry of the Cl_2 and its first solvation shell reveals that under high pressure the available volume in the trapping site has significantly decreased. In a small cage the molecule collides frequently with the walls. These repeated kicks give rise to the regular oscillations seen in Fig. 2. The frequency of this motion (≈ 35 cm^{-1}) is a clear signature of the locking effect and should be experimentally measurable. At intermediate pressures we have observed a gradual evolution from jump rotation at 12.5 kbar (the molecule jumps from one equilibrium well to another), to more and more hindered rotation at 25 and 50 kbar.

We now turn to the photodissociation process. The molecule is instantaneously brought to the repulsive $^1\Pi_u$ state where it attempts to dissociate. At each pressure value, 200 trajectories were run. We measure the reaction probability as the number of trajectories leading to well-separated photofragments (final and stable distance $\geqslant 5.5$ Å), when the system has come back to equilibrium. The value of 5.5 Å roughly corresponds to the distance between the center of two adjacent interstitial octahedral sites in the lattice, the sites where the photofragments are trapped when permanent separation of the photofragments has indeed occured. Over such distances the interaction between the fragments is negligible. Computational tests have shown that the aforementioned criterion is indeed a good signature of "permanent" dissociation. The results are summarized in Table II. As we see, the reaction probability strongly depends on the pressure. The former dramatically decreases from 30% to 2% between 0 and 12.5 kbar and the pressure threshold for photofragment separation should probably be found around 15–20 kbar. It is encouraging to note that these results agree with the experimental data of Katz and Apkarian.[13]

TABLE II. Photodissociation quantum yield as a function of the pressure. The temperature is 100 K.

$P_{(kbar)}$	0	12.5	25	50	100
$\phi_{(\%)}$	30	2	0	0	0

It is important to correlate between the pressure threshold for photodissociation and the rotational states of the molecule prior to excitation. Already in the case of zero pressure, when the varying parameter was the temperature, we have seen that the larger the deviations of θ from equilibrium, the higher the probability for the photofragments to escape the reagent cage. This is due to the fact that only certain orientations of the Cl_2 axis in the site are favorable for direct exit, since the molecule has to point towards a "window" in the potential in order to dissociate efficiently, otherwise the Cl/Xe collisions lead to deactivation of the Cl and finally will result in recombination. Only when free rotation is reached, these windows become easily accessible and reaction can proceed. As the pressure increases, two things occur. First the rotation becomes more and more hindered, which limits the chances to access the exit windows, but also these windows become smaller as the volume of the cage decreases. This fact explains why even at 12.5 kbar, when the rotation is not yet completely hindered, the reaction probability is already very low.

Finally, we have calculated for each pressure value the time evolution of the autocorrelation function of a unit vector along the Cl–Cl axis. We denote this unit vector by $\mathbf{r}(t)$. This correlation function describes the extent, at each time, to which polarization of the dissociating molecule is preserved. $\langle \mathbf{r}(0) \cdot \mathbf{r}(t) \rangle$ is shown in Fig. 3. Basically, this function tells us how much the Cl_2 bond remembers its initial orientation during the photodissociation process and after the recombination has occured. Figure 3 shows that as the pressure increases the molecule recombines in the same orientations that it was before the photoexcitation. At 12.5 kbar there is about 50% loss of memory, while at 100 kbar the initial orientation is almost fully conserved. This information should be directly extracted from experiments that measure the polarization of the recombinant emission: those molecules that do not dissociate, recom-

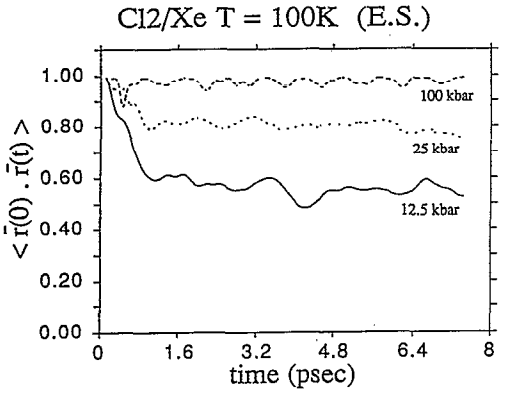

FIG. 3. The time evolution of the vector autocorrelation function at three different pressures.

bine, and relax radiatively via the $A' \rightarrow X$ emission.[12] When the dissociative absorption is excited by polarized radiation, if no rotation occurs during the dissociation/recombination process, then the recombinant emission should be polarized. The first generation of such experiments have already been conducted. At 100 K, and 50 kbar, residual polarization is observed.[25] The quantitative interpretation of this result is not yet complete, however, the qualitative interpretation is clear: the molecule retains memory of its initial orientation during the dissociation recombination process.

IV. CONCLUSIONS

In this paper we have presented classical trajectory results on the photodissociation dynamics of Cl_2 in crystalline xenon under high-pressure conditions. We found that the reaction probability strongly decreases as the pressure increases, in full agreement with previous experimental measurements. This effect is mainly due to the hindrance of the rotation of the halogen molecule in its trapping site prior to photoexcitation. The pressure also affects the size of the "window" in the cage potential through which photofragment exit from the cage can occur. Both effects play a role in the pressure dependence of the photodissociation quantum yield. Finally, we have proposed theoretical predictions for another aspect or the pressure influence, namely, the increased conservation of the initial orientation after the photoexcitation has taken place. The available experimental data supports this prediction. Quantitative comparisons require more data.

Finally, this study provides further indication how useful high pressure may be in controlling and studying reaction dynamics in molecular solids. Further experiments that explore the role of this thermodynamic variable and of other thermodynamic and dynamical parameters are strongly called for.

ACKNOWLEDGMENT

This research was supported by the U.S.—Israel Binational Science Foundation (Grant No. 88-00082), and by the Institute for Surface and Interface Science, University of California, Irvine, California. R. B. G. acknowledges support in the framework of the Saeree K. and Louis P. Fiedler Chair of Chemistry at The Hebrew University. The Fritz Haber Research Center is supported by the Minerva Gesellschaft für die Forschung, mbH, Munich, Germany.

[1] R. Alimi, R. B. Gerber, and V. A. Apkarian, J. Chem. Phys. **89**, 174 (1988).
[2] J. G. McCaffrey, H. Kunz, and N. Schwentner, J. Chem. Phys. **96**, 2825 (1992).
[3] R. Alimi, R. B. Gerber, and V. A. Apkarian, J. Chem. Phys. **92**, 3551 (1990).
[4] W. Lawrence, F. Okada, and V. A. Apkarian, Chem. Phys. Lett. **150**, 339 (1988).
[5] M. E. Fajardo, R. Whitnall, J. Feld, F. Okada, W. Lawrence, L. Wiedeman, and V. A. Apkarian, Laser Chem. **9**, 1 (1988).
[6] R. Alimi, R. B. Gerber, and V. A. Apkarian, Phys. Rev. Lett. **66**, 1295 (1991).
[7] R. Alimi, R. B. Gerber, H. Kunz, J. G. McCaffrey, and N. Schwentner, Phys. Rev. Lett. **69**, 856 (1992).
[8] R. Alimi, A. Brokman, and R. B. Gerber, J. Chem. Phys. **91**, 1611 (1989).
[9] R. Alimi, R. B. Gerber, and V. A. Apkarian, Chem. Phys. Lett. **158**, 257 (1989).
[10] M. E. Fajardo and V. A. Apkarian, J. Chem. Phys. **85**, 5660 (1986).
[11] M. E. Fajardo and V. A. Apkarian, Chem. Phys. Lett. **134**, 51 (1987).
[12] V. E. Bondybey and C. J. Fletcher, J. Chem. Phys. **64**, 3724 (1976); V. E. Bondybey and L. E. Brus, *ibid.* **65**, 620 (1975); **64**, 3724 (1976).
[13] A. I. Katz and V. A. Apkarian **94**, 6621 (1990).
[14] M. P. Allen and D. J. Tildesley, *Computer Simulation of Liquids* (Clarendon, Oxford, 1987).
[15] S. Nose, Mol. Phys. **52**, 255 (1984).
[16] H. C. Andersen, J. Chem. Phys. **72**, 2383 (1980); J. M. Haile and H. W. Graben, *ibid.* **73**, 2412 (1980).
[17] D. J. Evans and G. P. Morris, Chem. Phys. **77**, 63 (1983); D. J. Evans and G. P. Moriss, Phys. Lett. **98A**, 433 (1983)
[18] H. J. C. Berendesen, J. P. M. Postma, W. F. Van Gusteren, A. Di Nola, and J. R. Haak, J. Chem. Phys. **81**, 3684 (1984).
[19] J. A. Barker, R. O. Watts, J. K. Lee, T. P. Schafter, and Y. T. Lee, J. Chem. Phys. **61**, 3081 (1974).
[20] A. D. Booth, *Numerical Methods*, 3rd ed. (Butterworth, London, 1972).
[21] M. L. Klein and J. A. Venables, *Rare Gas Solids* (Academic, London, 1976).
[22] G. Herzberg, *Spectra of Diatomic Molecules*, 2nd Ed. (Van Nostrand, New York, 1950).
[23] S. D. Peyerimhoff and R. J. Buenker, Chem. Phys. **57**, 279 (1981).
[24] C. H. Becker, J. J. Valentini, P. Casavecchia, S. J. Sibener, and Y. T. Lee, Chem. Phys. Lett. **61**, 1 (1979).
[25] G. J. Hoffman, E. Sekreta, and V. A. Apkarian, Chem. Phys. Lett. **191**, 401 (1992).